IOP Conf. Series: Materials Science and Engineering **101** (2015) 012041 doi:10.1088/1757-899X/101/1/012041

Engineering, Manufacture and Preliminary Testing of the ITER Toroidal Field (TF) Magnet Helium Cold Circulator

C Rista, P.E.[1], J Shull[2], and S Sargent[3]

[1] Sales Engineer, Barber-Nichols Inc., 6325 W. 55th Ave., Arvada, Colorado 80002 USA
[2] Sr. Sales Engineer, Barber-Nichols Inc., 6325 W. 55th Ave., Arvada, Colorado 80002 USA
[3] Aero/Hydraulic Design Engineer, Barber-Nichols Inc., 6325 W. 55th Ave., Arvada, Colorado 80002

E-mail: CRista@Barber-Nichols.com

Abstract. The ITER cryodistribution system provides the supercritical Helium (SHe) forced flow cooling to the magnet system using cold circulators. The cold circulators are located in each of five separate auxiliary cold boxes planned for use in the facility. Barber-Nichols Inc. has been awarded a contract from ITER-India for engineering, manufacture and testing of the Toroidal Field (TF) Magnet Helium Cold Circulator. The cold circulator will be extensively tested at Barber-Nichols' facility prior to delivery for qualification testing at the Japan Atomic Energy Agency's (JAEA) test facility at Naka, Japan. The TF Cold Circulator integrates features and technical requirements which Barber-Nichols has utilized when supplying helium cold circulators worldwide over a period of 35 years. Features include a vacuum- jacketed hermetically sealed design with a very low helium leak rate, a heat shield for use with both nitrogen & helium cold sources, a broad operating range with a guaranteed isentropic efficiency over 70%, and impeller design features for high efficiency. The cold circulator will be designed to meet MTBM of 17,500 hours and MTBF of 36,000 hours. Vibration and speed monitoring are integrated into a compact package on the rotating assembly with operation and health monitoring in a multi-drop PROFIBUS communication environment using an electrical cabinet with critical features and full local and network PLC interface and control. For the testing in Japan and eventual installation in Europe, the cold circulator must be certified to the Japanese High Pressure Gas Safety Act (JHPGSA) and CE marked in compliance with the European Pressure Equipment Directive (PED) including Essential Safety Requirements (ESR). The test methodology utilized at Barber-Nichols' facility and the resulting test data, validating the high efficiency of the TF Cold Circulator across a broad operating range, are important features of this paper.

1. Introduction

Extended shaft cryogenic cold circulators are used in the cryogenics industry for many common applications involving liquid nitrogen, argon, hydrogen, and helium and supercritical helium. Typically, hydrogen and helium applications involve the use of vacuum jackets and optimized shaft extensions to reduce heat leak to the process fluid. Equipment common to cold circulator use include coldboxes and cryostats of many sizes and features.

For the ITER cryodistribution system, there will be five auxiliary cold boxes (Cryopump - CP, Central Solenoid - CS, Correction Coil - PF&CC, Structure - ST, and Toroidal Field Magnet - TF), each requiring a cold circulator to provide forced flow cooling of the magnet system with supercritical helium (SHe). The TF Cold Circulator is the subject of this paper. The performance requirements for the TF Cold Circulator are demanding with 70% guaranteed efficiency over a broad range of flow. Figure 1 shows a simplification of the ITER cryogenic system with SHe cold circulators.

2. Cold Circulator Features

Typical requirements for applications involving Cold Circulators include:

- Vacuum Jacket
- Hermetic Design
- Extended Shaft
- Inducer

- Easily Removable Rotating Assembly
- Motor Winding Temperature Sensors
- Extended Shaft Heat Station (Thermalization) for reduced Heat Leak
- Long Life Bearings using Low Vapor Pressure Cryogenic Bearing Greases
- Speed Pick-Up and Indication
- Vibration Sensors
- Speed Control by Variable Frequency Drive (VFD)
- Radiation Hardened including ancillary equipment (Sensors, Cables etc.)
- High Working Pressures (MAWP)
- Remote control via a specific communication protocol
- Guaranteed design & off-design performance and efficiency
- Anti-Icing Features
- Hour Usage Meter
- Start-Stop Counter
- Remote and Local PLC Control
- Anti-Thermal Acoustic Oscillation (TAO) Features
- Instrumentation and Control Cabinet for integrated power and control interlock

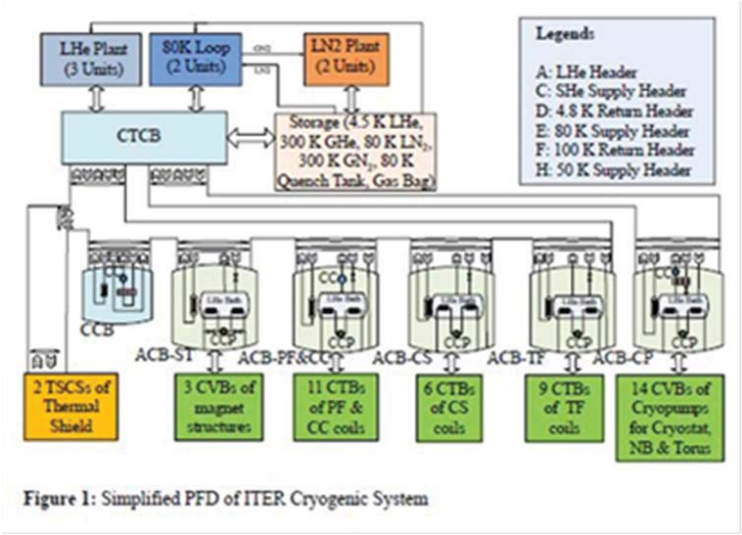

Figure 1. Simplified ITER Cryogenic System (Courtesy of ITER-India).

2.1 ITER TF Cold Circulator Requirements

Barber-Nichols has been manufacturing cold circulators for over 35 years to these typical requirements and features. The program for the ITER TF Cold Circulator is the first time that Barber-Nichols has had to implement virtually all of these features into a cold circulator design. A photo of the completed ITER TF Cold Circulator is shown in Figure 2 and 3:

Figure 2. ITER TF Cold Circulator Features - Vacuum Housing Removed.

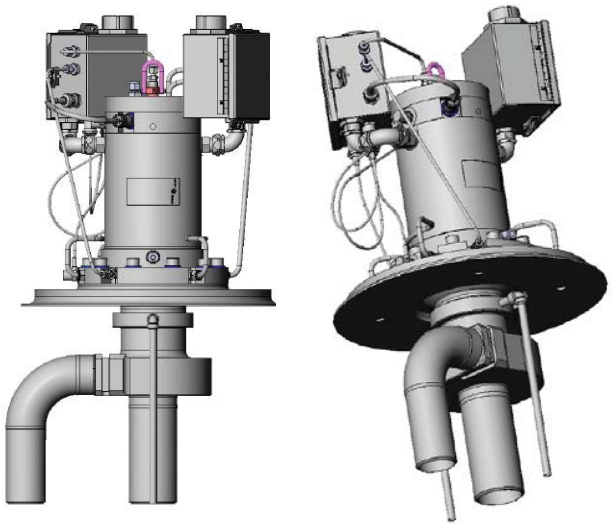

Figure 3. ITER TF Cold Circulator Features.

3. TF Cold Circulator Performance

The focus subject of this paper is the approach used to achieve a 70% guaranteed efficiency threshold over a wide operating range and the preliminary test results of the TF Cold Circulator design. Problems and issues were encountered and overcome during preliminary testing at Barber-Nichols' facility to confirm that the required performance guarantee efficiency points have been met. Further, the test results validate the design approach taken, which has been a first for Barber-Nichols to apply these concepts to a Supercritical Helium, cryogenic, vacuum-jacketed, extended shaft cold circulator. The methods used improved the performance potential of the full emission impeller and volute. These concepts used are typically applied in rocket turbopumps. Figure 4 performance curves show that the five (5) operational guarantee points have been preliminarily met after design, testing, and hardware mitigations at BNI's facility.

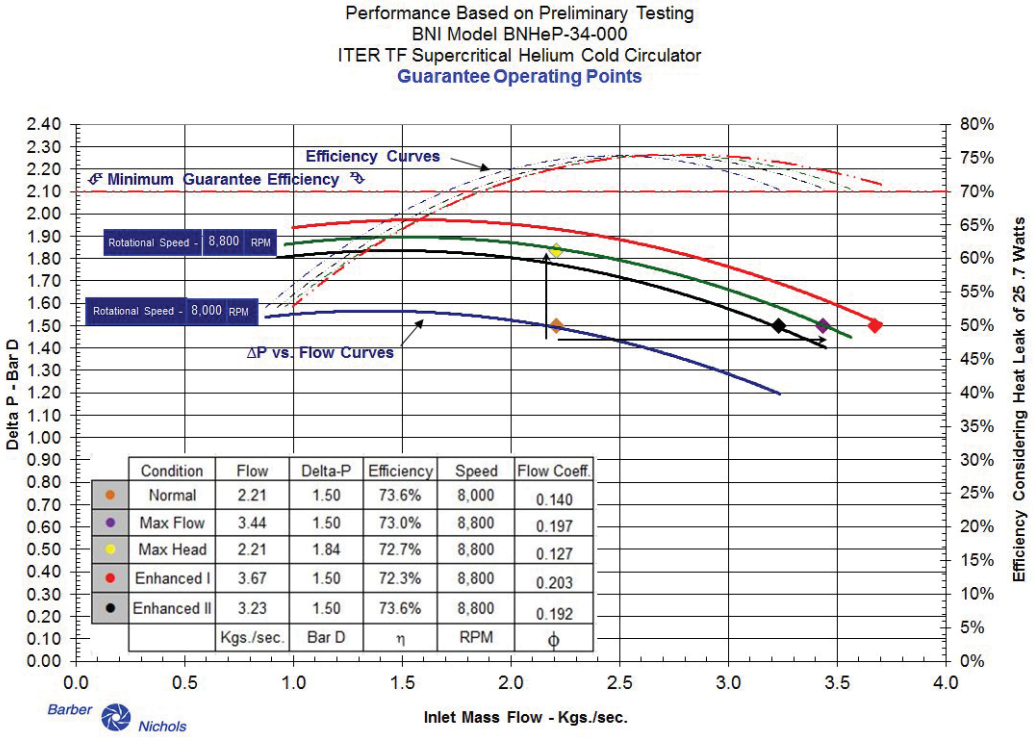

Figure 4. Preliminary Test Results for ITER TF Cold Circulator.

4. Overview of Principles Used in the Cold Circulator Design

Specific Speed, N_s, is defined as

$$N_s = \frac{N\sqrt{Q}}{\Delta H^{3/4}} \tag{1}$$

where N is the shaft speed in RPM, Q is the pump volumetric flow in gallons per minute (GPM), and ΔH the pump head rise in feet.

The head and flow of the pump are expressed in terms of their non-dimensional values, head coefficient (ψ) and flow coefficient (ϕ). This allows test data to be easily used in dimensionless analysis and to be used to characterize a pump or cold circulator which will be operated at different shaft speeds, and for analyzing changing cold circulator conditions and resulting performance. TF Cold Circulator flow coefficient is defined as the ratio of the impeller discharge meridional velocity C_m to the impeller tip speed, U. Pump head coefficient is defined as the pump head rise, ΔH, normalized by the impeller tip speed and gravitational constant.

$$\phi = \frac{C_m}{U} \tag{2}$$

$$\psi = \frac{\Delta H}{\left(\frac{U^2}{g}\right)} \tag{3}$$

TF Cold Circulator efficiency,η, is calculated from the TF Cold Circulator shaft power, Ps, head rise, ΔH, mass flow, m-dot, and unit conversion factor, f.

$$\eta = \frac{\text{m-dot x } \Delta H}{\text{Ps x } f} \tag{4}$$

Pumps are generally designed to achieve peak efficiency at the rated design or normal operation flow coefficient. Operation at other than the design flow coefficient (off-design operation) results in a decrease in efficiency (Figure 5). The steepness of the efficiency curve drop-off tends to increase as pump geometry and performance variables are optimized on very high performing machines such as rocket turbopumps.

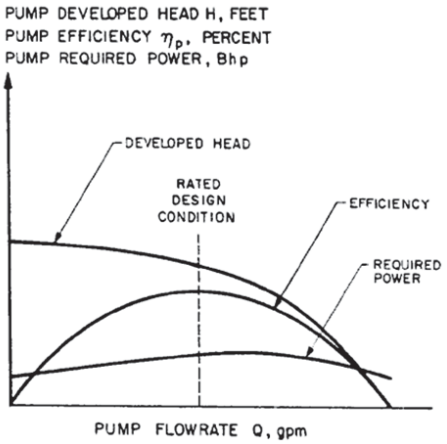

Figure 5. Typical Pump Performance Curves from Huzel and Huang [1].

The design, analysis, and test of the TF Cold Circulator required broadening the effective efficiency range beyond traditional applications. The end result is shown in Figure 4 where the best efficiency point (BEP) does not occur at what is specified as the 'Normal' operating point which is usually treated as the design point and the BEP.

The TF Cold Circulator design effort had to achieve a total to static stage efficiency of 70% or greater from the Normal Flow point with a flow coefficient of 0.140 up to a flow coefficient 41% higher for the Maximum Flow point ($\phi = 0.197$).

Expansion of the cold circulator's operating range by means of enlarging the discharge volute throat provided a simple approach along with ease of implementation to provide greater flow range for the higher mass flow operation. The design approach increased the risk of flow separation at low flow and at the Nominal condition. A depiction of a typical centrifugal volute throat, a key area of optimization in the TF Cold Circulator design, is shown in Figure 6:

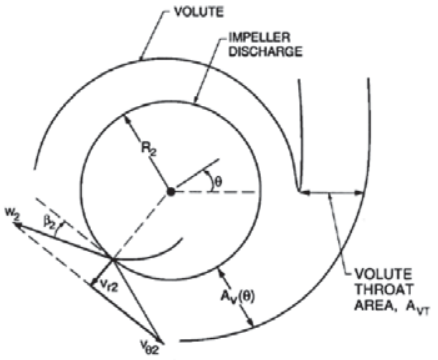

Figure 6. Typical Centrifugal Pump Volute as depicted in Brennen [2].

Initial speed selection for the TF Cold Circulator was made to maximize the efficiency potential. Pump specific speed, Ns, provides a convenient design parameter to assess the influence of pump speed on efficiency.

Examination of representative specific speed versus efficiency curves indicated that good efficiency potential occurs at the selected shaft speed for the TF Cold Circulator design condition of 8,000 RPM. Based on the pump flow rate of 253 GPM (2.21 Kg/s) and a resulting N_s value of 1,531 (in GPM, RPM, feet units), the BEP was be expected to be approximately 74%. The value is to be corrected for expected conductive and convective heat leak.

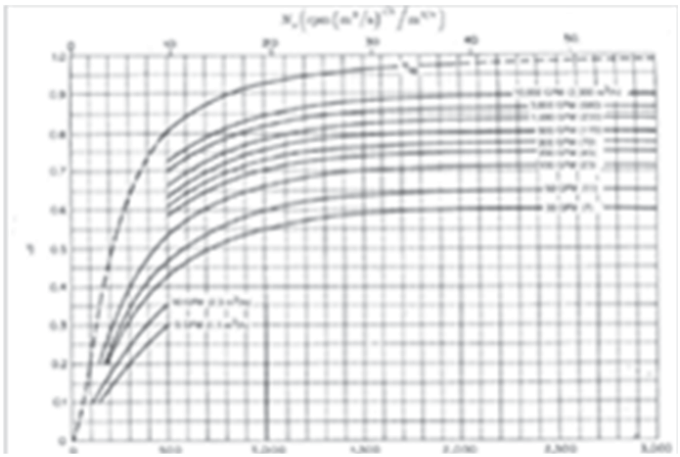

Figure 7. Efficiency potential vs N_s for pumps of various flow rates as found in Japikse [3].

4.1 Impeller Design

Trade studies to identify areas of impeller efficiency potential were performed with an internally developed 1-D pump design tool. Barber-Nichols' pump design tool employs distributed loss models utilizing correlations from BNI's past experience, as well as based on the works of Balje [4], Pfleiderer [5], Brennen [2] and others. The effects of discharge blade angle on efficiency were examined for volumetric flow and speed variations. Discharge flow angle was optimized allowing the impeller to produce the required head. The impeller optimization reduced skin friction losses through the impeller, increasing efficiency. The optimized impeller discharge traded with the impeller passage diffusion factor as the factor approached its practical limit. There were associated pressure losses adversely impacting efficiency. Mitigation to a fully optimized impeller design was also related to a discharge blade angle that posed manufacturing challenges. The physical result of the impeller optimization based on Ns and the trade studies are shown in Figure 8.

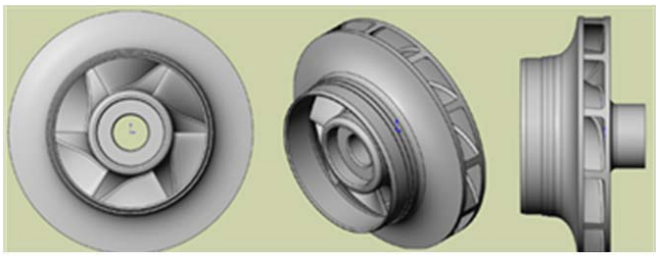

Figure 8. Impeller geometry based on N_s and trade studies.

4.2 Volute Design

The success of the chosen strategy for high efficiency over a wide flow range depended on the ability of BNI's prediction tools to account for the off-design behavior of the volute. In order to minimize the risk of flow separation in the volute, it is desired to increase the volute throat area by the minimum amount necessary to achieve the objective of near peak efficiency between flow coefficient (ϕ) values

of 0.140 (Normal) and 0.197 (Maximum Flow). This effectively shifted the TF Cold Circulator BEP from the Normal Flow point to approximately 2.5 Kg/s.

BNI accounted for the sudden expansion of the flow from the impeller discharge into the larger cross sectional area of the volute (the Borda-Carnot loss) and performed momentum mixing loss analysis to capture the loss of the fluid radial momentum. BNI's skin friction loss modeled the interaction of the fluid with the volute walls. The model output indicated acceptable efficiency at the desired high-end flow coefficient of 0.197 with the throat area increase. With the throat area defined, the subsequent volute area schedule is defined by means of a conservation of angular momentum based methodology such as that found in Karassik [6].

4.3 Stage Design

Although the interaction of impeller and volute had been modeled as one-dimensional, the detailed stage design and analysis was performed with computational fluid dynamics (CFD) to give higher fidelity definition to the interaction between the impeller and the volute.

The ANSYS CFX solver is used for the stage simulations. The mesh for the model for the TF Cold Circulator consists of unstructured tetrahedrons with approximately 5.7 million nodes with boundary layer inflation mesh. A steady state solution with a frozen rotor stage boundary condition is used for the interface between the rotating impeller and the stationary volute housing. Frozen rotor does not perform circumferential averaging of the flow field and is considered most appropriate for solutions with a large degree of asymmetry such as with the volute cut water, where there is a flow path nonconformity at the point the volute passage has rotated approximately 360 degrees around the impeller. A total of 4 solutions over the desired flow coefficient range were performed.

The streamlines through the pump volute are shown in Figure 9. No areas of large recirculation are present and the flow appears well behaved. The impeller in the figure is shaded with pressure contours.

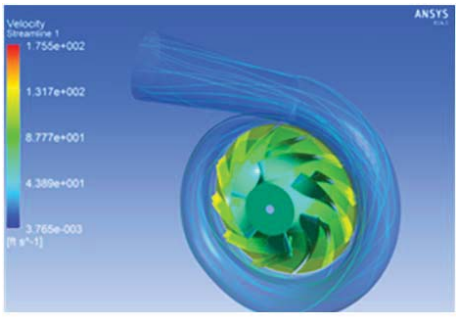

Figure 9. Streamlines through the volute at the design condition.

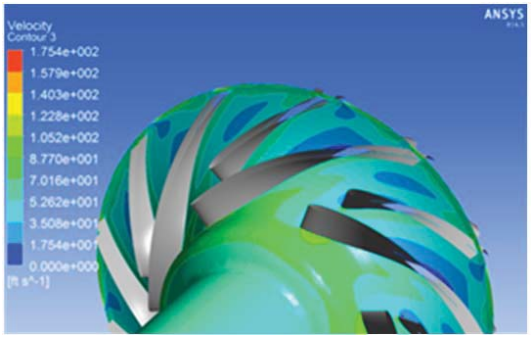

Figure 10. Impeller mid-span velocity contours at the the design condition.

In Figure 10, the velocity contours of the impeller are shown on the mid-span surface. Note the low velocity regions present near the suction side of the main impeller blades (lighter shaded

regions). Such velocity distributions are present in centrifugal pumps of all types and are caused by the interaction of the rotating channel fluid motion with centripetal force. The goal is to prevent fluid recirculation from occurring. Further analysis of the relative velocity vectors confirmed that the fluid is not recirculating, thus maintaining efficiency by minimizing flow angle deviation and pressure loss through the impeller.

5. Discussion of Test Results and Mitigations

Testing of the TF Cold Circulator was conducted in BNI facilities using a cold nitrogen recirculation loop. An electric motor with a variable frequency drive (VFD) was used to control the speed of the cold circulator. Calibration of the motor assembly was done using a dynamometer. This allowed for accurate power measurements for calculation of the cold circulator efficiency based on the measured power, which allowed calculation of efficiency with equation (4).

Test data results are shown in Figure 11 and Figure 12. The cold circulator was tested at two different speeds and with two different values of the impeller front shroud labyrinth clearance. Figure 11 indicates that the head coefficient from the test data is lower than that predicted by both the 1-D tool and by CFD analysis. There is good agreement between the test data and predictions made for the highest values of flow coefficients, with greater divergence occurring as the flow coefficient values decrease. The shape of the test data characteristic is similar to that of the CFD prediction, with a shallow, low slope from flow coefficient values of approximately 0.05 to 0.11. This behavior appears to indicate flow separation in the volute and a lack of static pressure recovery. As the flow increases and nears the design point, the test curve assumes a more positive slope suggesting that the volute is functioning as intended over these higher flow coefficient values. Even though this behavior was a known risk due to the enlargement of the volute throat and was given due attention in BNI's analysis, the magnitude of the volute performance shortfall was not accurately captured in the TF Cold Circulator Aero / Hydraulic design effort.

From a predictive standpoint, it appears that while the 1-D and CFD are in relative agreement for all head coefficient values for flow coefficients near Normal design flow and higher, a marked divergence in head coefficient prediction for flow coefficients lower than the design point is present. This appears to indicate that the 1-D tool is not able to fully predict the onset of flow separation in the volute and accurately predict the resulting performance impacts. The CFD seems to capture the presence of separation because the CFD curve shape agrees with the test data. The CFD analysis appears to underestimate the impact on head. It is unknown if this is due to an unsteady simulation or if a mesh refinement in the volute would aid in the prediction accuracy.

Test data taken at a larger value of impeller front shroud labyrinth seal clearance does not have a marked effect on the head coefficient performance. This appears to be further evidence that at this clearance, the volute is failing to recover static pressure from the impeller discharge as opposed to a pressure loss influenced by the larger impeller shroud seal clearance.

The efficiency data from Figure 12 shows that the desired objective was achieved, accommodating near peak efficiency from the range of flow coefficient of 0.140 to 0.197; an increase of 41% in flow coefficient with an efficiency reduction of 3 points from the BEP over this range. In contrast, a range given by a flow coefficient reduction of 40% was considered (in the range of 0.085 to 0.140), showing an efficiency reduction of up to 9 points.

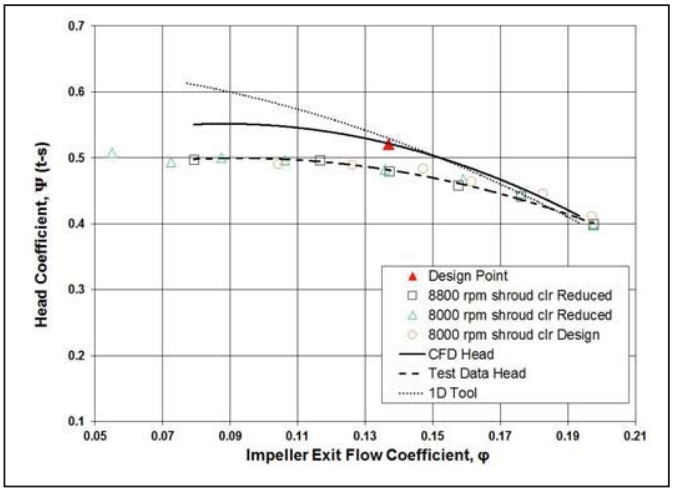

Figure 11. Head coefficient vs. flow coefficient results taken at two different speeds comparing values of impeller shroud clearance together with 1-D and CFD predictions.

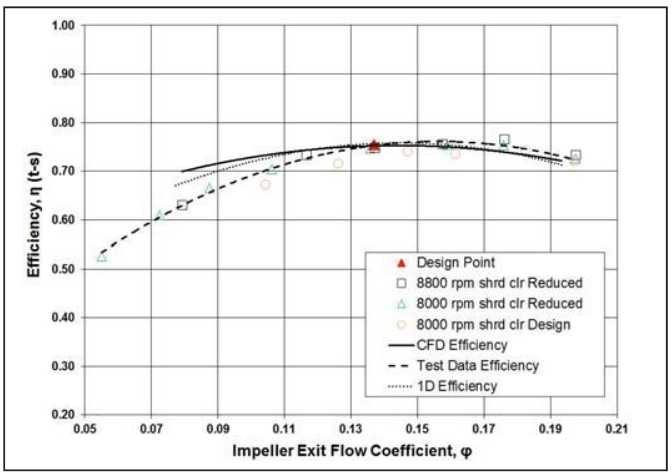

Figure 12. Efficiency vs. flow coefficient results taken at two different speeds comparing and values of impeller shroud clearance together with 1-D and CFD predictions.

5.1 Mitigation for Low Flow Coefficient Efficiency

As BNI expected, the mitigation to the decrease in efficiency in the low flow range was to decrease the impeller front shroud leakage flow by decreasing the front shroud labyrinth seal clearance. This change had a measurable and positive impact on the TF Cold Circulator efficiency. The parasitic losses associated with the front shroud leakage were minimized by the change in the seal clearance.

The efficiency predictions made from 1-D and CFD analysis agree well with the data at the Normal Flow coefficient value and above. For flow coefficient values lower than design, both the 1-D and CFD tools over predicted efficiency.

6. Summary and Conclusions

Preliminary testing of the ITER TF Supercritical Helium Cold Circulator indicates that the machine will meet its primary design objective of 70% efficiency over a very broad range of flow. Enlarging the volute throat above the nominal design value by a factor of 1.16 permits a large operating flow range near peak efficiency.

As expected, the design methodology undertaken comes at the expense of the volute pressure recovery at lower than the design (Normal Flow) coefficient. The test data obtained suggests

that great care must be taken in the analysis of the volute diffuser and to realize the potential for possible diffuser flow separation when looking to broaden cold circulator flow and peak efficiency.

Detailed analysis of the impeller, impeller and volute interaction, and the diffuser geometry is recommended. The successful results were supported by trade studies related to shaft speed evaluation of the specific speed parameter with variation of pump overall efficiency. These trades assisted in clarifying consideration of the impeller discharge blade angle and selection of the the design head coefficient (ψ). A volute loss model that considers the Borda-Carnot loss, momentum mixing loss, skin friction loss, and conical diffuser loss was used for the 1-D trade studies performed.

The comparisons of the preliminary test data with the predictions made with 1-D and CFD analysis provide insights into sources of head loss as well as areas of analysis requiring further attention.

References

[1] Huzel DK and Huang DH, 1967 *Design of liquid propellant rocket engines*, NASA **SP-125**
[2] Brennen CE, 1994 *Hydrodynamics of pumps*, Oxford University Press
[3] Japikse D Marscher WD and Furst RB, 1997 *Centrifugal pump design and performance*, Concepts ETI
[4] Balje, OE, 1981 *Turbomachines*, John Wiley & Sons
[5] Pfleiderer C, 1961 *Die kreiselpumpen für flüssigkeiten und gase, fünfter auflage*, Springer-Verlag
[6] Karassik IJ, Messina JP, Cooper P and Heald CC, 2001 *Pump handbook, third edition*, McGraw-Hill